

Measurement of the Critical Parameters and the Saturation Densities of Dimethyl Ether

Jiangtao Wu,* Zhigang Liu, Bin Wang, and Jiang Pan

State Key Laboratory of Multiphase Flow in Power Engineering, Xi'an Jiaotong University, Xi'an, Shaanxi 710049, People's Republic of China

On the basis of the direct visual observation of the meniscus disappearance and reappearance in an optical cell, 17 saturated liquid densities and 8 saturated vapor densities of dimethyl ether were measured in the temperature range from 301.816 K to the critical temperature, corresponding to a density range from (66.75 to 654.54) $\text{kg}\cdot\text{m}^{-3}$. The maximum uncertainties of the saturated liquid and vapor densities are $\pm 0.15 \text{ kg}\cdot\text{m}^{-3}$ and $\pm 0.10 \text{ kg}\cdot\text{m}^{-3}$, respectively. The uncertainties of temperature were estimated to be within $\pm 5 \text{ mK}$. The critical temperature T_c and density ρ_c were determined as $(400.378 \pm 0.005) \text{ K}$ and $(272 \pm 2) \text{ kg}\cdot\text{m}^{-3}$ by taking into consideration the meniscus disappearance and reappearance as well as the intensity of the critical opalescence. The critical pressure was $(5356 \pm 10) \text{ kPa}$ extrapolated from the vapor pressures data with the Wagner equation. We have also determined the critical exponent β and the critical amplitude B on the basis of a correlation of the vapor–liquid coexistence curve.

Introduction

Recent investigations of clean alternative fuels have shown that dimethyl ether and its mixtures have excellent properties as diesel fuels¹ and have a promising future as a replacement for fuels obtained from fossil reserves.^{2,3} Especially in China, the government offers support and funding for the synthesis of dimethyl ether and the development of automobile using dimethyl ether. Up to now, researchers have made considerable progress in the automobile fueled by dimethyl ether. In addition, dimethyl ether, as a chemical raw material, plays an important role in the synthesis of chemicals and is often used as an aerosol propellant, fuel additive, and liquefied petroleum gas substitute. Hence, reliable experimental thermophysical properties data of dimethyl ether are very urgent and indispensable.

In previous publications, the liquid viscosities, surface tensions, vapor pressures, and PVT data of dimethyl ether were reported.^{4–7} This paper reports measurements of the saturation densities in the near-critical region and the critical temperature and density. In addition, the critical exponent β and the critical amplitude B of dimethyl ether were determined, and a vapor–liquid coexistence curve correlation was developed.

Experimental Section

Materials. The sample of dimethyl ether was provided by Zhongshan Fine Chemical Co., Ltd. The mass purity is better than 99.95%, as indicated by analysis with gas chromatography (made by Dongxi Instruments Corp. in China, model GC-4000A). A thermal conductivity detector (TCD) was used on analysis with the carrier nitrogen at 30 mL/s, and the column temperature and the oven temperature are 383 K and 423 K, respectively. Hence, no further purification was processed in this work.

Apparatus. The experimental apparatus used for the measurements was originally developed by Wang et al.⁸ and is similar to the apparatus reported by Okazaki et al.⁹ To improve the accuracy, some modifications were made, the mass of the cell was decreased, and the inner surface was polished. The apparatus was remanufactured before this experiment.

The experimental schematic diagram is shown in Figure 1. It consists of an optical cylindrical sample cell with two quartz glass windows at both ends for observing the meniscus, a thermostatic bath, and a temperature measurement system. The cell was made of 304 stainless steel and installed in the thermostat bath. The inner volume of the cell was determined with pure water, and the process was repeated three times. The final value was $(11.6114 \pm 0.0005) \text{ cm}^3$ at 290.9 K. The details of the thermostat bath and temperature measurement have been described in refs 10 and 11. Thus, only a brief introduction will be given here.

The temperature in the thermostat bath can be varied from (220 to 550) K. The temperature stability and uniformity depend on the anticipated temperature range and the selected bath fluid. In the present work, the temperature stabilities are better than $\pm 3 \text{ mK}$ over an hour, and the 201–10# methyl-silicon oil was used as bath fluid. Temperature was measured with a high-precision thermometry bridge F18 (made by ASL in UK) and a 25- Ω standard platinum-resistance thermometer (No. 92822). The thermometer was calibrated from (273.15 to 933.473) K on the ITS-90 scale with an uncertainty of $\pm 0.65 \text{ mK}$ in the temperature range of this work at the National Institute of Metrology of China. The measurement accuracy of F18 is better than $\pm 0.1 \text{ ppm}$. The total uncertainty of temperature measurement is better than $\pm 1 \text{ mK}$. During the experiment, the standard platinum-resistance thermometer was installed as near as possible to the optical cell.

Procedure. The saturation densities in the vicinity of the critical point were measured by direct observation of

* To whom correspondence may be addressed. Email: jtwu@mail.xjtu.edu.cn. Fax: 86-29-82668789.

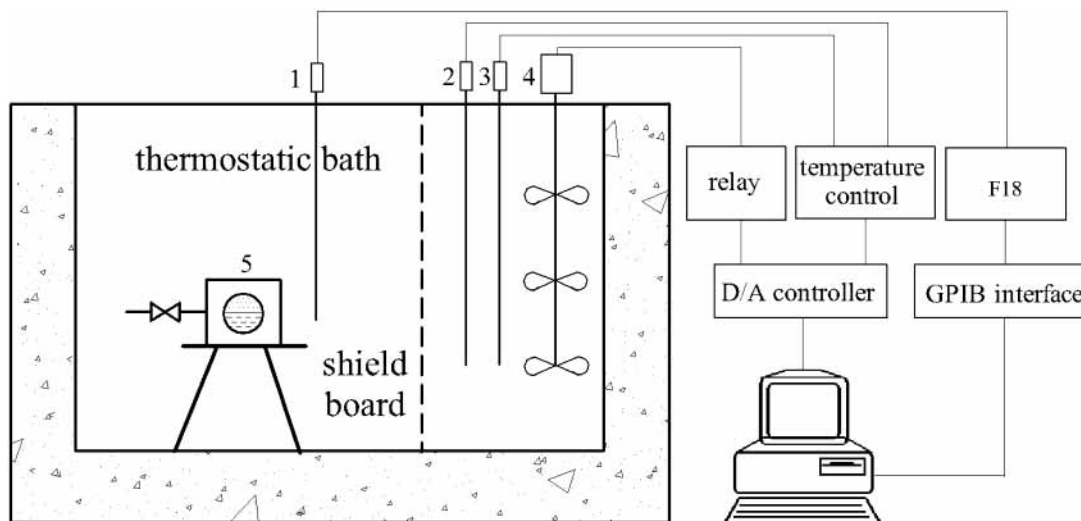


Figure 1. Schematic diagram of experimental apparatus. 1, 25 Ω SPRT; 2, auxiliary-heater; 3, controlled heater; 4, stirrer motor; 5, apparatus.

the meniscus (vapor–liquid coexistence interface) disappearance (or reappearance) and critical opalescence. The critical opalescence is observed when fluids become colored dark brown or black in the critical region (including critical point).

The density of the sample in the optical cell was calculated from the mass of the sample, which was weighted on a precision standard balance (0.5 mg, Shanghai, TG31B) and the known volume of the cell. To maintain the accuracy of results, the apparatus was cleaned carefully and weighed more than three times at intervals of 10 min before or after each measurement. When the meniscus disappears at the top of the cell, or disappears in the cell and critical opalescence of the vapor phase is more intense than of the liquid phase, the average sample density in the optical cell was the saturated-liquid density and is greater than the critical density. When the meniscus disappears at the bottom of the cell or disappears in the cell and critical opalescence of the liquid phase is more intense than of the vapor phase, the average sample density in the optical cell was the saturated-vapor density and is lower than the critical density.

The saturation temperature along the vapor–liquid coexistence curve for a specified density was determined by observing the meniscus disappearance, when the meniscus disappears at the top or bottom of the cell. If the meniscus disappears in the optical cell, the saturation temperature has to be determined by observing the meniscus reappearance from the supercritical state to the subcritical state, otherwise the value of saturation temperature will be little larger than the true value. The detail explanation was given in ref 11.

After each saturation temperature measurement, the sample in the cell was discharged and refilled to change the sample density, and then the saturation temperature was measured again. In addition, special attention was paid to establish a uniform temperature for a certain period of time in order to maintain a well-established thermal equilibrium condition.

Results

Seventeen saturated liquid densities and eight saturated vapor densities of dimethyl ether were determined in the vicinity of the critical point, and the results were given in Table 1. The range of densities is from (66.75 and 654.54) $\text{kg}\cdot\text{m}^{-3}$, and the maximum uncertainties of the saturated

Table 1. Saturation Liquid and Vapor Densities of Dimethyl Ether

T/K	$\rho_{\text{exp}}/\text{kg}\cdot\text{m}^{-3}$	T/K	$\rho_{\text{exp}}/\text{kg}\cdot\text{m}^{-3}$
301.816	654.54	400.323	299.12 ^a
320.083	623.90	400.349	285.01 ^a
330.634	604.34	400.362	278.92 ^a
339.469	585.82	400.377	276.19 ^a
347.338	567.13	400.378	272.05 ^a
358.996	540.45	400.361	264.02 ^a
365.688	522.25	400.349	253.84 ^a
372.151	503.13	399.344	203.55
378.807	479.19	396.059	161.30
384.495	454.66	390.864	130.05
393.654	405.87	380.954	96.42
398.210	361.58	366.695	66.75
399.662	334.06		

^a Density values obtained when the critical opalescence was observed.

liquid and vapor are $\pm 0.15 \text{ kg}\cdot\text{m}^{-3}$ and $\pm 0.10 \text{ kg}\cdot\text{m}^{-3}$, respectively. The uncertainties of the temperature depend on the temperature stability of the thermostat bath, the uncertainty of the temperature measurement, and the individual error with respect to the determination of the meniscus-disappearing or meniscus-reappearing temperature. The total standard uncertainty of the temperature is estimated to be within $\pm 5 \text{ mK}$.

The critical opalescence was observed at 7 measurements for the densities between (253.84 and 299.12) $\text{kg}\cdot\text{m}^{-3}$. These measurements are given with an asterisk for the measured density values in Table 1. For 13 saturated liquid densities above 334.06 $\text{kg}\cdot\text{m}^{-3}$, the meniscus ascended with increasing temperature and disappeared at the top of the optical cell. For 5 saturated vapor densities below 203.55 $\text{kg}\cdot\text{m}^{-3}$, the meniscus descended with increasing temperature and disappeared at the bottom of the optical cell. At measurements near the critical density, the meniscus disappeared without reaching either the top or bottom of the optical cell. From the critical opalescence, it was determined if the density of the cell belongs to saturated liquid density or vapor density.

Critical Parameters. The critical state is characterized by critical opalescence at an overall density close to the critical density. By increasing the temperature very slowly from the subcritical state to supercritical state, the meniscus disappears at the center of the optical cell. At the

Table 2. Coefficients of the Equation 4

	b_1	b_2	b_3	source
saturated liquid 1	1.506780	1.065007	-0.173841	this work
saturated liquid 2	1.523689	1.023972	0.270555	this work, ref 14
saturated vapor	-1.793180	0.134222	42.730198	this work

critical point, the critical opalescence is most intense and equal in both the vapor and liquid phase. By decreasing the temperature very slowly from the supercritical state to subcritical state, the appearance of the fluid changes from colorless to yellowish, reddish, completely black, reddish, yellowish, and colorless. At the critical point, we think the fluid should be completely black.

At the density of $276.19 \text{ kg}\cdot\text{m}^{-3}$, the critical opalescence in the vapor phase was observed more intensely than that in the liquid phase. At the density of $264.02 \text{ kg}\cdot\text{m}^{-3}$, the critical opalescence in the liquid phase was observed more intensely than that in the vapor phase. At the density of $272.05 \text{ kg}\cdot\text{m}^{-3}$, the intensity of the critical opalescence in both the liquid and vapor phase are very close. On the basis of these observations, the critical density value was determined to be

$$\rho_c = (272 \pm 2) \text{ kg}\cdot\text{m}^{-3} \quad (1)$$

The critical temperature was determined as the saturation temperature that corresponds to the critical density. Here, the critical temperature was determined by decreasing the temperature very slowly from the supercritical state, at the density of $272.05 \text{ kg}\cdot\text{m}^{-3}$. The temperature that corresponds to when the fluid appears completely black is considered as the critical temperature, as shown in Table 1

$$T_c = (400.378 \pm 0.005) \text{ K} \quad (2)$$

In this work, the critical pressure p_c was extrapolated from the Wagner vapor pressure equation covering the temperature range 233 to 398 K with the critical temperature T_c given at above. The uncertainty of the critical pressure depends on the uncertainty of the critical temperature and the accuracy and extrapolability of the vapor pressure equation. The critical pressure of dimethyl ether was determined to be

$$p_c = (5356 \pm 10) \text{ kPa} \quad (3)$$

The previously published critical parameters of dimethyl ether were already reviewed in the refs 12 and 13. Most of the data were obtained before the 1940s and have large differences. The results of Zawisza and Glowka¹³ (1970) are close to those of the present values and within the uncertainty of their results. The limited instruments and the purity of sample are the major reasons for deviations. The results of this work should be more reliable than previous measurements.

Correlations. The experimental results listed in Table 1 were correlated as a function of temperature using the following equation

$$\rho_r = 1.0 + b_1 \tau^\beta + b_2 \tau^{2\beta} + b_3 \tau^{1/\beta} \quad (4)$$

where $\rho_r = \rho/\rho_c$, ρ_c is the critical density ($272 \text{ kg}\cdot\text{m}^{-3}$), $\tau = 1.0 - T/T_c$, where T_c is the critical temperature (400.378 K), β is critical exponent (0.334, determined in the following), and b_1 , b_2 , and b_3 are fitting parameters, and the values for saturated liquid and saturated vapor of dimethyl

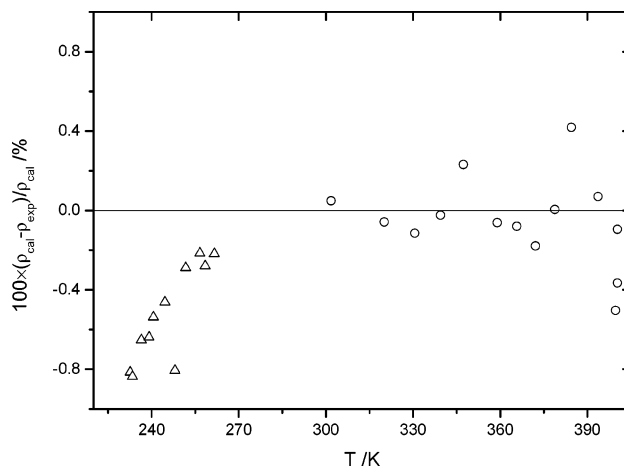


Figure 2. Deviations of the saturated liquid densities from eq 4 using the coefficients of saturated liquid 1. \circ , this work; \triangle , Maass and Boomer.

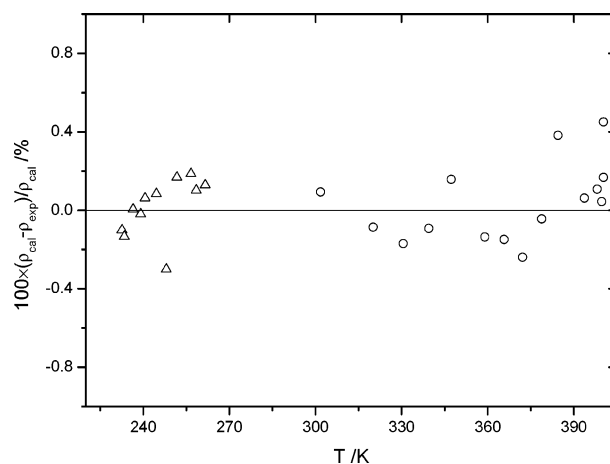


Figure 3. Deviations of the saturated liquid densities from eq 4 using the coefficients of saturated liquid 2. \circ , this work; \triangle , Maass and Boomer.

ether are listed in Table 2. The deviations of the saturated liquid densities from eq 4 by using the parameters of saturated liquid 1 are shown in Figure 2, and the average absolute deviation and maximal deviation are 0.13% and 0.35%, respectively. The average absolute deviation and maximal deviation of the saturated vapor densities from eq 4 are 1.4% and 4.8%, respectively.

Maass et al.¹⁴ have measured a few saturated liquid density data of dimethyl ether in the temperature range from (232 to 261) K. We have extrapolated the saturated densities from eq 4 by using the parameters of saturated liquid 1. The deviations are shown in Figure 2. The maximum deviation between the calculated value and published experimental value is less than 0.9%. The comparisons indicated that the present measurements and the measurements of Maass et al. agreed within the estimated uncertainty. Finally, the coefficients of eq 4 were fitted with all the available saturated liquid densities of dimethyl ether, as shown in Table 2 (saturated liquid 2). The deviations of the saturated liquid densities from eq 4 by using the parameters of saturated liquid 2 are shown in Figure 3, and the average absolute deviation and maximal deviation are 0.14% and 0.45%, respectively. Equation 4 with the saturated liquid 2 parameters was recommended to calculate the liquid density of dimethyl ether for it has more applicable temperature range than eq 4 with the saturated liquid 1 parameters.

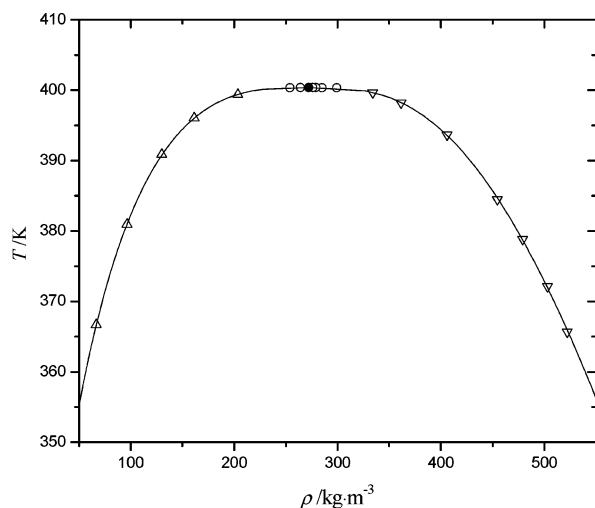


Figure 4. Vapor–liquid coexistence curve of dimethyl ether. ●, critical point; ○, coexistence point; ▽, saturated-liquid density; △, saturated-vapor density.

Table 3. Numerical Constants in Equation 6

D_0	D_1	D_2	B_0	B_1
-1.194332	2.625134	-0.360594	1.761741	0.345415

Discussion

The critical exponent β is essential for modeling the vapor–liquid coexistence curve in the critical region by means of the following power law representation

$$\frac{(\rho' - \rho'')}{2\rho_c} = B|\Delta T^*|^\beta \quad (5)$$

where $\Delta T^* = (T_c - T)/T_c$, ρ' is the saturated liquid density, ρ'' is the saturated vapor density, and B is the critical amplitude. Equation 5 requires isothermal pairs of liquid and vapor densities. Therefore, the following correlation for the calculation of a pair of saturated liquid and vapor densities was used

$$\Delta\rho^* = D_0|\Delta T^*|^{1-\alpha} + D_1|\Delta T^*|^{1.0} + D_2|\Delta T^*|^{1-\alpha+\Delta_1} \pm B_0|\Delta T^*|^\beta \pm B_1|\Delta T^*|^\beta + \Delta_1 \quad (6)$$

where $\Delta\rho^* = (\rho - \rho_c)/\rho_c$, $\Delta T^* = (T_c - T)/T_c$, and α and β are critical exponents. The exponent Δ_1 stands for the first symmetric correction-to-scaling exponent of the Wegner expansion. From the theoretical background of eq 6, these exponents are $\alpha = 0.1085$, $\beta = 0.325$, and $\Delta_1 = 0.50$. The critical parameters in eq 6 are those determined in this work, being $T_c = 400.378$ K and $\rho_c = 272$ kg·m⁻³. On the basis of the present measurements, the coefficients D_0 , D_1 , D_2 , B_0 , and B_1 were determined by the least-squares fitting, as shown in Table 3. In this least-squares fitting, 13 data points were used as a set of input data, by excluding 6 measurements (densities from (253.84 to 285.01) kg·m⁻³) in the close vicinity of the critical point corresponding to $|\Delta T^*| < 7.5 \times 10^{-5}$. The upper sign “+” and the lower sign “-” of the fourth and fifth terms in eq 6 correspond to the saturated liquid and vapor phases, respectively. Equation 6 is effective for the range of densities between (66.75 and 522.25) kg·m⁻³. The vapor–liquid coexistence curve calculated from eq 6 is shown in Figure 4. The deviations of the density measurements from eq 6 are illustrated in Figure 5. The average absolute deviation and maximum deviation are 0.15% and 0.53%, respectively. The results indicated that eq 6 could reproduce the input data well.

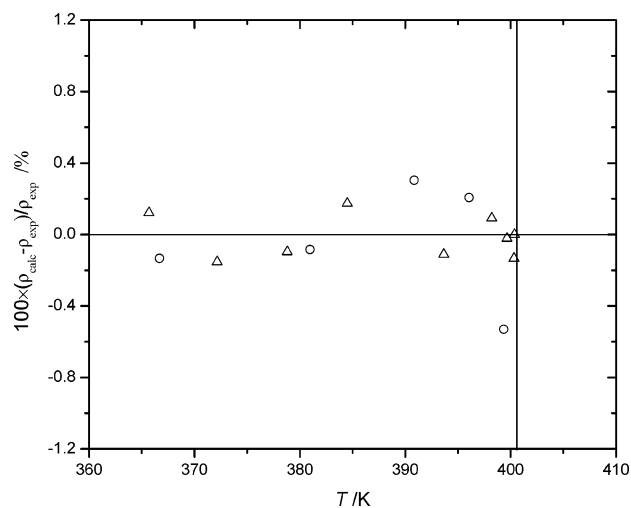


Figure 5. Deviations of the saturated liquid and vapor densities from eq 6. ○, saturated vapor density; △, saturated liquid density.

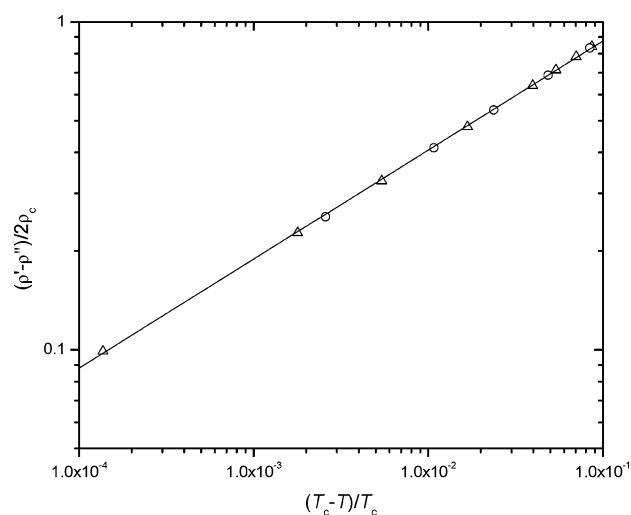


Figure 6. Critical exponent and amplitude of dimethyl ether. ○, saturated vapor density; △, saturated liquid density.

Figure 6 shows a logarithmic plot between $(\rho' - \rho'')/2\rho_c$ and $|\Delta T^*|$ in terms of the present measurements and calculated results from eq 6. The power-law representation, eq 5, suggests that the experimental results can be satisfactorily fitted by a straight line, and the slope of the straight line is equivalent to the critical exponent β . To determine the critical exponent β and the critical amplitude B , the data utilized for determination of the coefficients in eq 6 were used. As a result of the least-squares fitting, the values $\beta = 0.334$ and $B = 1.884$ were obtained. The β value is little greater than the theoretical value 0.325 calculated from the three-dimensional n -vector model ($n = 1$) via the renormalization group theory.^{15,16}

Conclusions

By means of visual observation of the meniscus in the optical cell, 25 saturated vapor and liquid densities of dimethyl ether in the critical region were measured and the critical parameters, the critical exponent β , and critical amplitude were determined. The correlations of saturated liquid and vapor densities for dimethyl ether were developed on the basis of the present measurements and other available results. The correlations are able to represent the experimental results within $\pm 0.5\%$ in the temperature 230 K to the critical temperature for saturated-liquid density.

Acknowledgment

This research is supported by the National Basic Research Priorities Program of Ministry of Science and Technology of China (973 Project, Grant No. 2001CB209208) and the National Natural Science Foundation of China (Grant Nos. 50336020, 50306021).

Literature Cited

- (1) Wang, H. W.; Zhou, L. B.; Jiang, D. M.; Huang Z. H. Study on the Performance and Emissions of a Compression Ignition Engine Fuelled with Dimethyl Ether. *Proc. Inst. Mech. Eng., Part D* **2000**, *214*, 101–106.
- (2) Hansen, J. B.; Voss, B.; Joensen, F.; Sigurdardottir, I. D. Large Scale Manufacture of Dimethyl Ether. A New Alternative Diesel Fuel from Natural Gas. SAE Paper No. 950063, 1995.
- (3) Kikkawa, Y. Dimethyl Ether Fuel Proposed as an Alternative to LNG. *Oil Gas J.* **1998**, *96*, 55–59.
- (4) Wu, J. T.; Liu, Z. G.; Bi, S. S.; Meng X. Y. Viscosity of Saturated Liquid Dimethyl Ether from (227 to 343) K. *J. Chem. Eng. Data* **2003**, *48*, 426–429.
- (5) Wu, J. T.; Liu, Z. G.; Wang, F. K.; Ren C. Surface Tension of Dimethyl Ether from (213 to 368) K. *J. Chem. Eng. Data* **2003**, *48*, 1571–1573.
- (6) Wu, J. T.; Liu, Z. G.; Pan, J.; Zhao X. M. Vapor Pressure Measurements of Dimethyl Ether from (233 to 399) K. *J. Chem. Eng. Data* **2004**, *49*, 32–34.
- (7) Wu, J. T.; Liu, Z. G.; Pan, J.; Wang, B. Burnett Measurement for Gas-Phase PVT of Dimethyl Ether from 298 to 353 K. *Fluid Phase Equilib.* **2004**, to be published.
- (8) Wang, J.; Liu, Z. G.; Tan, L. C.; Yin, J. M. Measurements of the Vapor-Liquid Coexistence Curve in the Critical Region for Refrigerant Mixture R152a/R22. *Fluid Phase Equilib.* **1992**, *80*, 203–211.
- (9) Okazaki, S.; Higashi, Y.; Takaishi, Y.; Uematsu, U.; Watanabe, k. Procedures for Determining the Critical Parameters of Fluids. *Rev. Sci. Instrum.* **1983**, *54*, 21–25.
- (10) Wu, J. T.; Liu, Z. G.; Huang H. H.; Pan J.; Zhao, X. M.; He, M. G. Development of New High Accuracy PVTx Measurement Experimental System. *Xi'an Jiaotong Daxue Xuebao* **2003**, *37*, 4–9.
- (11) Wu, J. T. Development of the New Thermophysical Properties Measurement System and Research of Thermophysical Properties of Dimethyl Ether. Ph.D. Dissertation, Xi'an Jiaotong University, 2003.
- (12) Kobe, K. A.; Lynn, R. E. The Critical Properties of Elements and Compounds. *Chem. Rev.* **1953**, *52*, 117–236.
- (13) Kudchadker, A. P.; Ambrose, D.; Tsonopoulos, C. Vapor-Liquid Critical Properties of Elements and Compounds. 7. Oxygen Compounds Other Than Alkanols and Cycloalkanols. *J. Chem. Eng. Data* **2001**, *46*, 457–479.
- (14) Maass, B. O.; Boomer, E. H. Vapor Densities at Low Pressures and over an Extended Temperature Range. I. The Properties of Ethylene Oxide Compared to Oxygen Compounds of Similar Molecular Weight. *J. Am. Chem. Soc.* **1922**, *44*, 1709–1728.
- (15) Guillou, J. C. L.; Zinn-Justin, J. Critical Exponents from Field Theory. *Phys. Rev. B* **1980**, *21*, 3976–3998.
- (16) Albert, D. Z. Behavior of the Borel Resummations for the Critical Exponents of the *n*-Vector Model. *Phys. Rev. B* **1982**, *25*, 4810–4814.

Received for review November 25, 2003. Accepted March 19, 2004.

JE034251+